

## **CHAPTER 2**

### **State of Knowledge**

#### **2.1. ASPHALT CEMENT**

Asphalt binder is defined by the American Society for Testing and Materials (ASTM) as a "dark brown to black cementitious material in which the predominating constituents are bitumens that occur in nature or are obtained in petroleum processing. As cement, asphalt is especially valuable to the pavement applications because it is strong, readily adhesive, highly waterproof, and durable (Asphalt Institute, 1997). It provides limited flexibility to mixtures of mineral aggregates. It is also highly resistant to the reaction with most acids, alkalis, and salts.

The applications of asphalt binder rely on its properties as a preservative, waterproofing, and adhesive agent, which were first recognized by the Egyptians and utilized throughout the Middle Ages. Even with the long history of asphalt usage, the evolution of asphalt as a widespread ingredient in paving material did not occur until modern petroleum-refining techniques were developed in the early 1900's. Since that time, and especially during the last 50 years, the proper utilization of its full potential has relied less on the pragmatic use of "Black Arts" and more on the application of the physical and chemical sciences.

##### **2.1.1. Production**

By far the most commonly used binder in the world today is petroleum bitumen. Crude petroleum is a mixture of compounds boiling at different temperatures that can be separated into a variety of generic fractions by distillation and by fractionation (Speight, 1994). Petroleum binder can be obtained by exposing the crude oil to atmospheric distillation followed by vacuum distillation. The vacuum distillation residue is the basic bitumen obtained from the refining process. The amount and type of bitumen obtained from the distillation depends on the crude oil origin and refining process. As presented in Figure 2.1, the amount and properties of residual of asphalt binder vary significantly from one source to another.

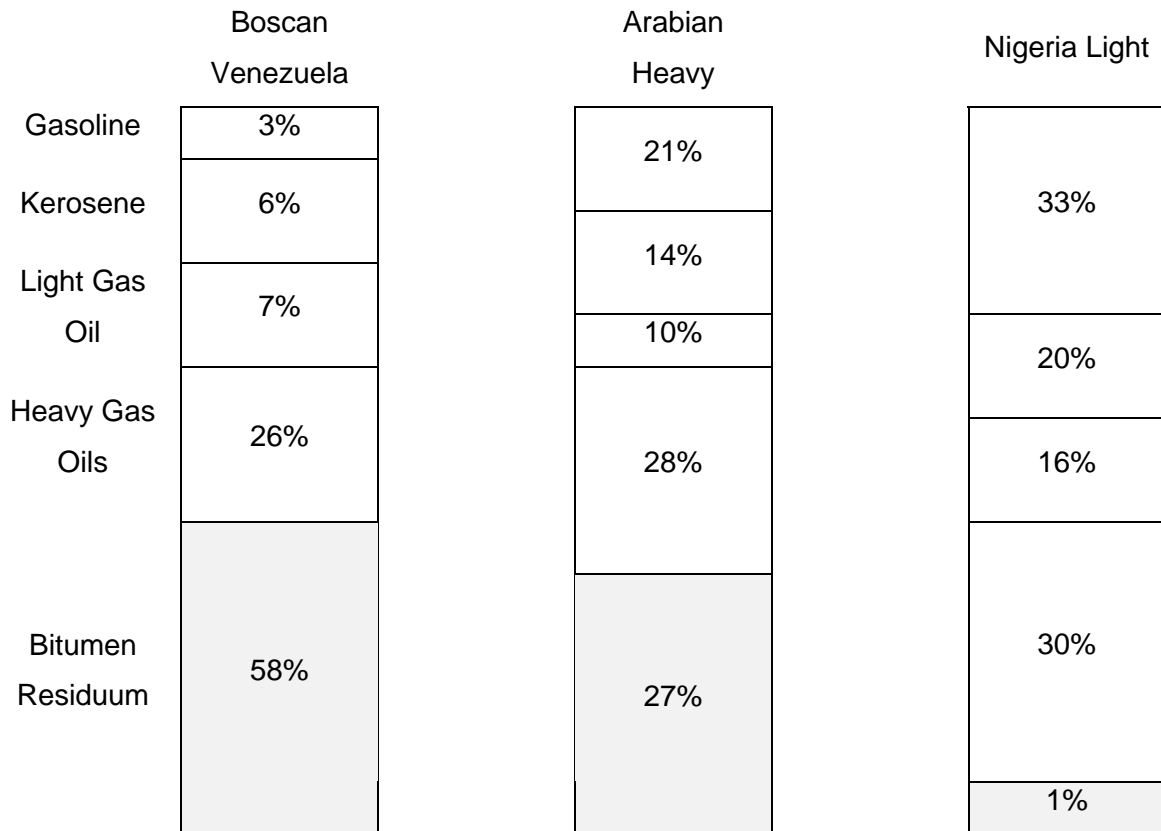


**Figure 2.1.** Composition of Crude Petroleum From Three Different Sources (after Roberts *et al.*, 1991)

Of 1500 different crude petroleums produced around the world, only 250 have been reported to be suitable for bitumen production (Nicholls, 1998). In many cases, different crude oils are mixed to produce an asphalt binder that falls within the required specifications (Corbett, 1984).

### 2.1.2. Structure and Chemistry of Asphalt Binders

The chemical structure of asphalt binder is very complex and consists of a variety of chemical compounds of high molecular weight, typically between 500 and 50,000. These variations are mainly due to the crude source and to the refining process. Because of its complexity, a complete analysis of the composition of asphalt binder would be almost impossible. However, although this wide variation in its molecular structure, 90 to 95% by weight of asphalt consists of carbon and hydrogen, which is why it is classified as a hydrocarbon. The remaining portion consists of two types of atoms:

heteroatoms and metals (Asphalt Institute, 1997). The heteroatoms, such as nitrogen, oxygen, and sulfur, although present in small percents, contribute to most of the chemical and physical properties of the binder by causing most of the interaction between molecules. Metal atoms, such as vanadium, nickel, and iron, are present in small quantities, usually less than one percent.

As presented in Table 2.1, the chemical composition of the binder varies significantly from one crude source to another. It is also affected by the aging status of the binder (Petersen, 1984).

**Table 2.1.** Elemental Analysis of Four Different Asphalt Binders (after Lewandowski, 1994).

Element	Composition			
	Mexican Blend	Arkansas	Boscan	California
<i>Carbon</i>	83.77	85.78	82.90	86.77
<i>Hydrogen</i>	9.91	10.19	10.45	10.93
<i>Nitrogen</i>	0.28	0.26	0.78	1.10
<i>Sulfur</i>	5.25	3.41	5.43	0.99
<i>Oxygen</i>	0.77	0.36	0.29	0.20
<i>Vanadium, ppm</i>	180.00	7.00	1380.00	4.00
<i>Nickel, ppm</i>	22	0.40	109.0	6.00

To investigate the composition of asphalt binder, asphalt components are separated using the difference in solubility between its various molecules. Two methods frequently used are Corbett's chromatographic method (ASTM D 4124, Standard Test Method for Separation of Asphalt into Four Fractions) and Rostler's precipitation method presented at the Proceedings of the Association of Asphalt Paving Technologists in 1962 (Rostler, 1962). The Corbett method uses differential absorption and desorption, while the Rostler method uses sulfuric acid of varying strength to analytically separate the different components. Both methods separate the involatile part, known as asphaltenes, using two different solvents (n-heptane or n-pentane). The asphaltenes are black amorphous solids, which are relatively rich in heteroatoms and more aromatic than the rest of the binder. Asphaltenes generally comprise 5 to 25% by weight of the binder. The remaining groups, resins and oils, are defined differently by each method.

Corbett refers to this mix as petrolenes, consisting of saturates, naphthene aromatics, and polar aromatics. Rostler refers to this mix as maltenes, composed of paraffins, first and second acidifins, and nitrogen bases.

### 2.1.3. Asphalt Models

To describe the asphalt binder chemical structure, several studies have proposed different models based on the investigation of asphalt binder components, especially the asphaltenes that can be easily isolated from crudes. In the early 1920s, Nellensteyn (1924) introduced the concept that petroleum residues are colloidal dispersions of asphaltenes in maltenes that represent the solvent phase peptized by polar materials called resins. Pfeiffer and Saal (1940) considered aromaticity gradients in their model and did not address distributions of heteroatom-containing molecules with polar functional groups. They noticed that asphalt properties are a function of the strength of associations between fundamental components of dispersed phases and the extent to which dispersed phases are peptized by solvent phases. Traxler (1961) studied this concept of colloidal model. He emphasized the rationalization of rheological properties of asphalts. In asphalt, in which the presumably high molecular weight asphaltenes are well dispersed, high temperature susceptibility, high ductility, low rate of age hardening, and little thixotropy should be observed. In poorly dispersed asphalt, low temperature susceptibility, low ductility, significant thixotropic property and rapid age-hardening rate are observed. Such asphalt is designated as gel-type. Most of the commercial binders are between these two extremes. He noticed that the phenomenon of isothermal, reversible age hardening that he called steric hardening, was strong evidence of the formation of secondary structures unstable to heat and mechanical agitation, and that asphalts are colloidal (Traxler and Coombs, 1937).

The colloidal model has been criticized because, although it appears appropriate, it is difficult to substantiate experimentally (Bukka *et al.* 1991). Recent attempts to characterize asphalt binder have led to the introduction of the micellar model presented in Figure 2.2, which is considered as a more appropriate colloidal model for presenting asphalt binder chemical structure. This model is a three-phase system consisting of a dispersed phase (asphaltenes), a continuous phase (oils), and a dispersant (resins) (SHRP, 1994).

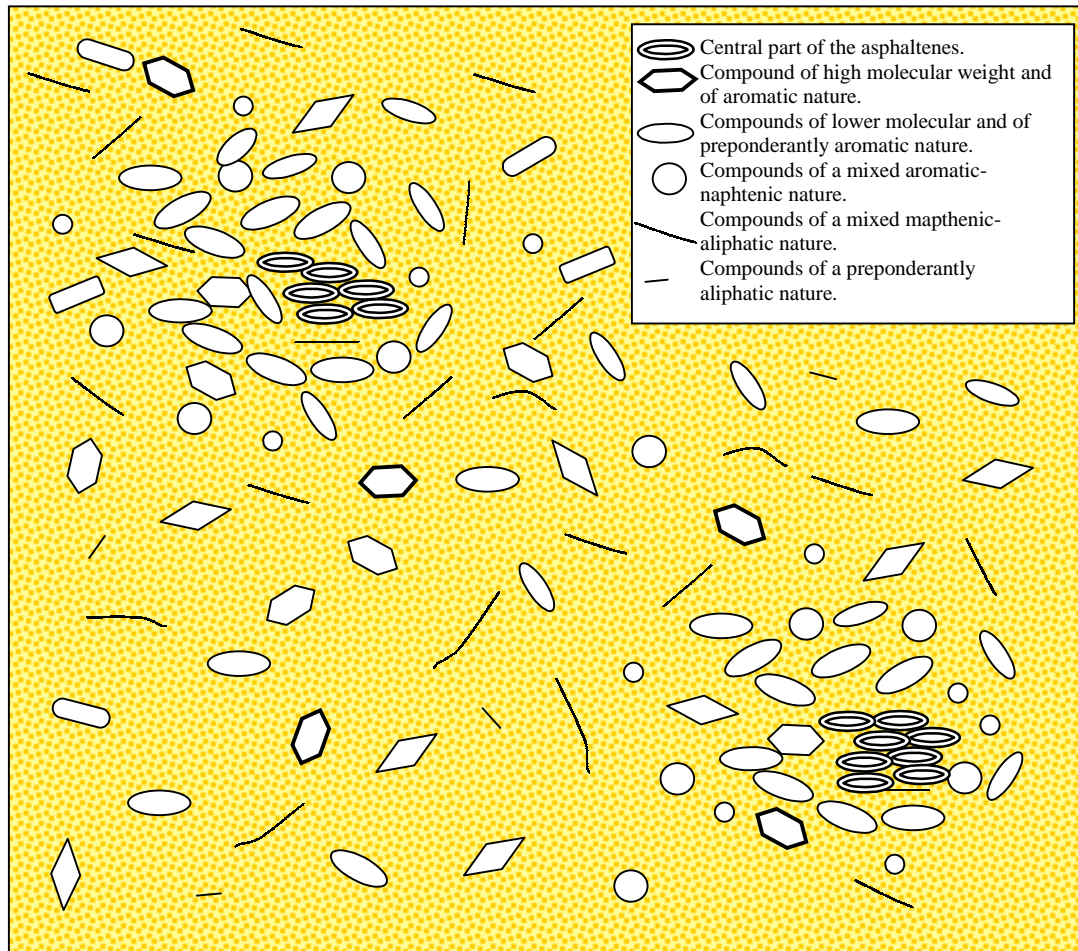


**Figure 2.2.** A Schematic of Micellar Model for Asphalt Binders (after Lewandowski, 1994)

During the Strategic Highway Research Program (SHRP), a complete review of the colloidal literature led to the conclusion that traditional colloidal systems are not fully consistent with the observed rheological behavior of asphalt binder as a function of temperature, loading time, and aging. A new microstructural model, derived from previous work done by Pfeiffer and Saal (1940), was proposed. According to this model, asphalt consists of a solvent phase composed of relatively aliphatic, nonpolar molecules that are low in heteroatoms, and dispersed microstructures consisting of more polar, aromatic, asphaltene-like molecules. Many of the molecules that compose the dispersed phase are assumed to be polyfunctional and capable of associating in primary microstructures through hydrogen bonds.

## 2.2. CONVENTIONAL ASPHALT BINDER TESTS

Because of its chemical complexity, asphalt specifications have been developed around physical property tests relevant to the performance of the binder. The traditional physical property tests are performed at standard test temperatures, and their results are used to determine whether the material meets the specification criteria. However, many of these tests are empirical and rely on previous experience to establish a suitable judgement for the material performance. This section presents a summary of the conventional consistency tests currently in use by many pavement engineers throughout the world.

Softening Point (ASTM D 36): Measures the temperature at which a disc of binder is unable to support a standard metal ball, indicating a change of state of the asphalt from semi-solid to liquid. The softening point is approximately an equiviscous temperature when binders have a viscosity of approximately 1200 Pa.s. (Nicholls, 1998). Although its use in binder specification is quite common in Europe, it is used mostly for high viscosity roofing asphalts in the United States.

Needle Penetration Test (ASTM D 5): Measures the consistency of asphalt binder by measuring the depth to which a standard needle will penetrate into a sample under a specified load at a specified temperature within a specific period of time (5 sec). Normally, the load is 100g and the temperature is 25°C (Figure 2.3).

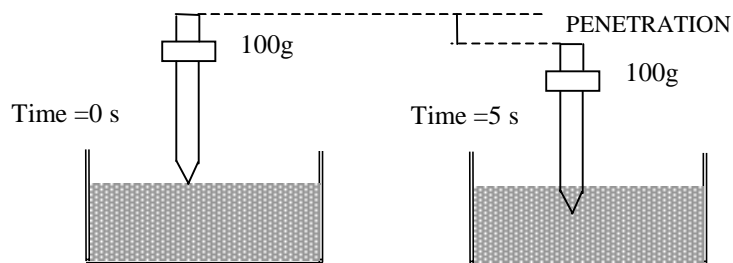


**Figure 2.3.** Penetration Test

Ductility (ASTM D113): Ductility is evaluated by measuring the distance in centimeters that a standard briquette of asphalt binder will stretch before breaking. The test is performed at a standard temperature of 25°C (77°F) in a water bath by separating the two ends at a rate of 50mm/min until rupture.

Viscosity (ASTM D 2170 and 2171): The viscosity is defined as the ratio of the shear stress to the shear strain rate and has units of P.sec (Nicholls, 1998) or simply the resistance of a fluid to flow. Two different viscosities are measured for asphalt binder: absolute and kinematic. The absolute viscosity is measured at a temperature of 60°C (140°F) using a U-shaped capillary tube viscometer. Asphalt binder is poured into the large tube of a viscometer, and it rises in the capillary tube under the application of a partial vacuum to the other side of the tube. The time required for the binder to flow between two marks on the tube is converted to a viscosity using calibration factors.

The kinematic viscosity test is performed at 135°C (275°F) using a Zeitfuchs Cross-Arm viscometer. At this temperature, asphalt binder is sufficiently fluid to flow through the capillary tube under its own weight. This temperature was selected because it is relatively close to the mixing temperature used in placement of the hot mix asphalt (HMA) layer. To obtain the dynamic viscosity, the time required for the binder to flow between two timing marks is multiplied by the calibration factor of the tube. Dynamic viscosity is usually expressed in unit of centistokes because gravitational forces induce flow and the density of the material affects the rate of flow. Compared to the other consistency tests, viscosity is a fundamental property that is independent of the sample size or the testing system.

### **2.3. SUPERPAVE™ ASPHALT BINDER TESTS AND SPECIFICATIONS**

Although the viscoelastic behavior of asphalt binder is too complicated to be described by simple empirical tests such as penetration and softening point, these consistency tests have served very well over the years for specifying binders. However, as a result of increasing traffic, axle loadings, and tire pressures, a new range of high performance road binders have been introduced that can have quite complex behavior compared to the traditional unmodified binders. These traditional tests cannot be used to characterize these newly developed binders. The consistency tests do not adequately

describe the linear viscoelastic properties that are needed to relate physical properties to performance, to relate asphalt chemistry to performance, and to develop a performance-related binder specification (SHRP, 1994). Table 2.2 presents the properties currently included in National Specifications for asphalt binder in selected countries throughout the world (after Nicholls, 1998).

**Table 2.2.** Properties in National Specifications for Asphalt Binder (after Nicholls, 1998).

Property	Country				
	UK	France	Germany	USA	Australia
Penetration at 25°C	Yes	Yes	Yes	Yes	----
Penetration at 15°C	----	----	----	----	Yes
Softening point	Yes	Yes	Yes	----	----
Fraass point	----	Yes	Yes	----	----
Ductility	----	----	Yes	Yes	----
Wax content	----	Yes	Yes	----	----
Ash content	----	----	Yes	----	----
Solubility	Yes^	Yes^	Yes^	Yes^	Yes^
Density	----	Yes	Yes	----	----
Flash point	----	Yes	----	Yes	Yes
Durability	----	----	----	----	Yes
Viscosity at 60°C	----	----	----	Yes	Yes
Viscosity at 135°C	----	----	----	Yes	Yes
RTFOT*	----	----	----	----	Yes
TFOT#	----	----	----	Yes	----
Loss on heating	Yes	Yes	----	----	----

\* RTFOT: Rolling Thin Film Oven Test

# TFOT: Thin Film Oven Test

^ Different solvents are specified

Recognizing the deficiencies in the traditional testing system for binders, in 1987, the Strategic Highway Research Program (SHRP) began developing new tests for measuring the physical properties of binder. A major result of this \$50 million research effort is the SuperPave™ (*Superior Performing Asphalt Pavements*) binder tests and specifications. The implementation of this system is moving at an adequate rate in the United States but it is facing a serious drawback in other parts of the world, especially Europe. According to European pavement engineers (Eurobitume, 1995), their decision to switch over to the SuperPave™ system would be conditioned by the following: Achieving at least the same level of reliability as their current system and establishing an appropriate link between the new system and the old one.

SuperPave™ asphalt binder technology is still in an emerging phase at this time (1999). Work is continuing on the evaluation and improvement of SuperPave™ with the ultimate objective of full nationwide implementation. Although much work remains to be done, a process of scientific evaluation has taken the industry to a thorough appreciation of both the difficulties and the advantages associated with the new system. The ability to accurately predict pavement performance in terms of permanent deformation, fatigue cracking, and thermal cracking is considered to be the only mechanism by which rational binder specifications, fundamental mix design procedures, economic justification for modified asphalt binders, improved structural design, and realistic performance-based quality specifications can be developed (University of Maryland, 1996). Different studies to test and validate the new system are underway. The next section presents a summary of the SuperPave™ physical tests for asphalt binders.

### 2.3.1. SuperPave™ Performance-Related Tests for Asphalt Binders

SuperPave™ focuses on controlling three types of pavement distress: permanent deformation and fatigue cracking as the main load associated distress, and low temperature cracking as one of the major non-load associated distresses. Material selection and mix design also consider the effects of aging and moisture sensitivity on the development of these types of distress (Zhang, 1996). The objective of the SuperPave™ mix design is to define an economical blend of asphalt binder and aggregate that results in a paving mixture having sufficient asphalt durability, air voids, workability, as well as satisfactory performance characteristics over the expected service life of the pavement (Cominsky, 1994).

The SuperPave™ binder specification introduced a new set of test equipment and procedures. Tests and specifications are intended for asphalt “binders”, including both modified and unmodified asphalt cements. The selection of a performance grade (PG) is based on the average seven-day maximum pavement design temperature and the minimum pavement design temperature. A unique feature of this system is that the specified criteria remain constant, but the temperature at which the criteria must be met changes for the various PG grades. The tests are performed at temperatures that are encountered by in-service pavements. Table 2.3 presents the list of testing equipment used by the SuperPave™ system.

**Table 2.3.** Equipment Used by the SuperPave™ Binder Specification

Equipment	Purpose
Rolling Thin Film Oven (RTFO)	Simulate binder aging during HMA production and installation.
Pressure Aging Vessel (PAV)	Simulate oxidative aging that occurs in the binder during pavement service life.
Rotational Viscometer (RV)	Measure binder handling and pumping properties during construction.
Dynamic Shear Rheometer (DSR)	Measure binder properties at high and intermediate service temperatures (performed on original binder, RTFO-aged binder, and PAV residue).
Bending Beam Rheometer (BBR)	Measures binder properties at low service temperatures.
Direct Tensile Tester (DTT)	Measures binder properties at low service temperatures (complementary test conducted if binder fails BBR criteria).

**Rolling Thin Film Oven (AASHTO T 240).** The rolling thin film oven (RTFO) aging procedure is a conditioning step that simulates construction aging of asphalt binders. The RTFO (Figure 2.4) consists of an oven chamber with a vertical circular carriage. Sample bottles rest in the carriage and the assembly rotates about the carriage center. A fan circulates air in the chamber. At the bottom of the rotation, an air jet blows hot air into the sample bottle.

Thirty five  $\pm$  0.5 g of asphalt binder is poured in each bottle and then placed in the carriage and rotated at a rate of 15 rev/min. The airflow is set at a rate of 4000 ml/min, and the samples are subjected to these conditions for 85 min. The conditions in the test are not exactly as found in the field but experience has shown that the amount of hardening in the RTFO test correlates reasonably well with that observed in a conventional batch mixer (Whiteoak, 1990).



**Figure 2.4.** Rolling Thin Film Oven

The RTFO test determines the mass of volatiles lost from the binder during the test. Volatile mass loss is an indication of the aging that may occur in the asphalt during mixing and construction operations. Mass loss is reported as the average percent loss of two samples after RTFO aging and is calculated using the following equation:

$$\text{Mass Loss, \%} = \frac{\text{Original mass} - \text{Aged mass}}{\text{Original mass}} \times 100 \quad (2.1)$$

The RTFO-aged asphalt binder is then used for dynamic shear rheometer (DSR) testing, transferred into PAV pans for additional aging, or equally proportioned into small containers and stored for future use.

**Pressure Aging Vessel (AASHTO Provisional Method PP1).** This method is designed to simulate the oxidative aging that occurs in asphalt binders during pavement service by means of pressurized air and elevated temperature. This test accounts for temperature effects but is not intended to account for mixture variables such as air voids, aggregate type, and aggregate adsorption (SHRP, 1994). Residue from this test may be used to estimate the physical or chemical properties of binder after five to ten years of aging in the field. The Pressure Aging Vessel (PAV) is presented in Figure 2.5. This test is conducted by placing the asphalt binder in a heated vessel pressurized with air to  $2.1 \pm 0.1$  MPa for 20 hrs. The temperature of the test is varied depending on the climate in which the binder will be used. A temperature range of 90 to 110°C is used to simulate conditions ranging from cold mountain to hot desert regions.



**Figure 2.5.** Pressure Aging Vessel

The aging process is simulated by the combination of elevated temperature and the pressure that forces oxygen into the asphalt binder, thereby accelerating the oxidative aging process.

**Dynamic Shear Rheometer (AASHTO TP5).** This test is used to measure the linear viscoelastic moduli of asphalt binders in a sinusoidal loading mode. Measurements may be obtained at different temperatures, strain and stress levels, and test frequencies. The Dynamic Shear Rheometer (DSR) operation is simple; asphalt binder is sandwiched between two parallel plates, one that is fixed and one that oscillates.

As the plate oscillates, the sample is subjected to a defined strain or stress that is resisted by the material through its complex shear modulus ( $G^*$ ). The complex shear modulus ( $G^*$ ) is a measure of the total resistance of a material to deformation when exposed to repeated pulses of shear stress (Asphalt Institute, 1997). Figure 2.6 illustrates the theory of operation of the DSR with  $\delta$  representing the phase angle in degrees between the applied stress and the resulting shear strain.

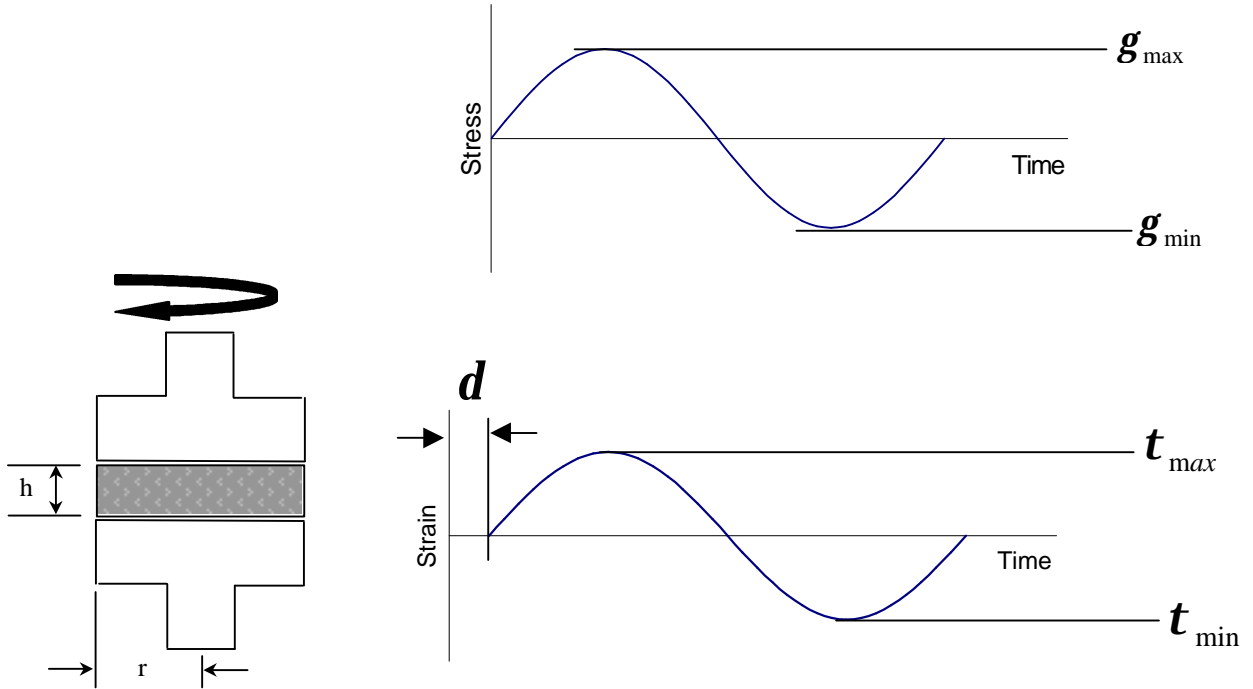


**Figure 2.6.** Operation Principle of the Dynamic Shear Rheometer

The applied stress and resulting strain are defined as follows:

$$t = 2T / \pi r^3 \quad (2.2)$$

$$g = q r/h \quad (2.3)$$

where,

$\tau$  is the applied shear stress (Pa);

T is the applied torque (N.m);

r is the radius of the sample (m);

h is the thickness of the sample (m);

$\theta$  is the resulting deflection angle (rad); and

$\gamma$  is the resulting shear strain (%).

The complex shear modulus,  $G^*$ , can then be calculated as follows:

$$G^* = (t_{\max} - t_{\min}) / (g_{\max} - g_{\min}) \quad (2.4)$$

Dynamic shear test may be conducted in two ways: controlled-stress and controlled-strain. A controlled-stress test applies a sinusoidally varying stress and measures the magnitude and phase of the resulting strain. A controlled-strain test applies a sinusoidally varying strain to the sample and measures the magnitude and phase of the resulting stress. Figure 2.7 shows a typical DSR instrument



**Figure 2.7.** Dynamic Shear Rheometer

A DSR system consists of three major parts: the rheometer, the controller, and the computer. Three types of test are performed during this study for the dynamic shear testing: strain sweeps, frequency sweeps, and stress viscometry. Strain sweeps are used to determine the region of linear behavior. In this case, the stress level is gradually increased until significant non-linearity is detected in the response. Frequency sweeps are used to measure the complex shear modulus ( $G^*$ ) and the phase angle  $\delta$  at different temperatures by applying a defined strain and a sweep of frequencies allowing construction of the master curves for the binder under consideration. The stress viscometry option is used to calibrate the temperature by measuring the viscosity of a known viscosity fluid and determining the equipment performance.

Two sample sizes are used, depending on the testing temperature: a sample with a 25-mm-diameter and a thickness of 1 mm is used for high temperatures (46 to 82°C)

and a sample with an 8-mm diameter and a thickness of 2 mm is used for intermediate temperatures (4 to 40°C).

There are three different methods for preparing the sample for DSR testing:

- Pouring hot asphalt binder on the lower plate. Hot asphalt binder may be poured directly into the lower plate of the rheometer.
- Preforming a sample in a silicone mold. Hot asphalt binder may be poured into a silicone rubber mold and allowed to cool to room temperature. The sample is then removed from the mold and placed on the lower plate of the rheometer.
- Pouring hot asphalt binder on the upper removable plate. Hot asphalt binder may be poured directly into the upper plate at room temperature; the upper plate being removed from the rheometer.

Sample preparation has been found to play an important role in getting repeatable results (Francken, 1997). Precasting the samples in flexible molds, as recommended by SHRP, has proven to be the most efficient way to achieve this goal. As shown in Figure 2.8, the use of molds may result in a better centering of the sample, which highly affects the repeatability of the results (Maccarrone *et al.*, 1995).

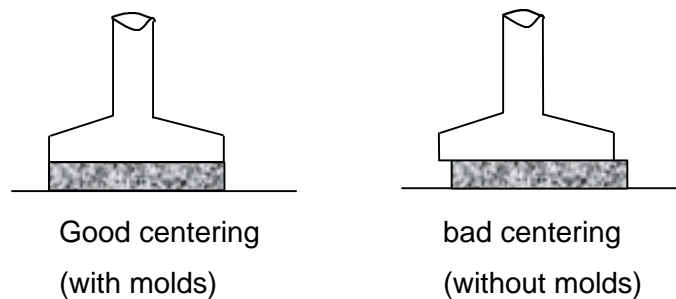


**Figure 2.8.** Repeatability of the Results for Sample Preparation (after Maccarrone *et al.*, 1995)

**Bending Beam Rheometer (AASHTO TP1).** The Bending Beam Rheometer (BBR) is used to measure the low-temperature creep response of asphalt binders. The BBR test temperatures are related to the pavement's lowest service temperature, when the binder behaves more like an elastic material. The temperature usually ranges from -40 to 25°C depending on the grade and aging history of the binder. Figure 2.9 illustrates the main

components of the BBR system. The key elements of the BBR are a loading frame, temperature-controlled fluid bath, and the computer control and data acquisition system.



**Figure 2.9.** Bending Beam Rheometer

The BBR is operated by applying a constant load at the midspan of an asphalt beam that is simply supported (supported at its two ends and loaded at the center). During the test, the deflection of the center point of the beam is measured continuously. The asphalt beam is supported at both ends by stainless steel half-rounds that are 102mm apart. The specimen, the supports, and the lower part of the test frame are submerged in a constant-temperature fluid bath, which controls the test temperature. Figure 2.10 illustrates the loading system out of the fluid bath for clarification.

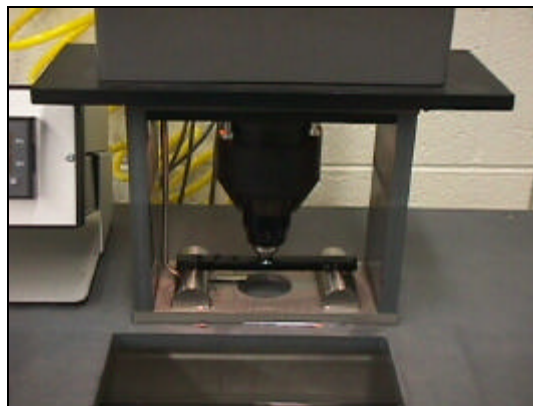


**Figure 2.10.** Loading System in the BBR

The loading unit in the device consists of an air bearing and a pneumatic piston that controls the movement of the loading shaft. The loading shaft serves a dual purpose: its upper end is attached to a linear variable differential transformer (LVDT) that precisely

measures the shaft movement, and its own weight is used to apply the required load on the sample. The magnitude of the load is controlled by adjusting the pressure in the pneumatic piston. By applying a constant load to the asphalt beam and measuring the center deflection of the beam throughout the four-minute test procedure, the creep stiffness (S) and creep rate (m) can be calculated. The creep load simulates thermal stresses that gradually build-up in a pavement when temperature drops. Creep stiffness is the resistance of the asphalt binder to creep loading and the m-value is the change in asphalt stiffness with time during loading (Asphalt Institute, 1997). The m-value is the slope of the log stiffness versus log time curve at any time, t. Using the beam theory, it can be shown that the creep stiffness at loading time t can be calculated as follows:

$$S(t) = PL^3/4bh^3\delta(t) \quad (2.5)$$

where,

S(t) is the creep stiffness of the binder at loading time t (MPa);

P is the constant applied load (N);

L is the span length (mm);

b is the width of the beam (mm);

h is the depth of the beam (mm); and

$\delta$  is the time-dependent deflection of the beam at midspan (mm).

The desired value of creep stiffness is when the sample has been loaded for two hours at the minimum pavement design temperature. However, using the concept of time-temperature superposition, it was found that by raising the test temperature 10°C, an equal creep stiffness can be obtained after only a 60 sec loading.

#### **2.4. POLYMER MODIFIED BINDER**

In recent years, an increase in traffic loading including, axle load, tire pressure, and number of passes, has shown some limitation in asphalt binder performance. Although asphalt binder has performed satisfactorily on a wide range of roads in the past, dramatic failures in hot-mix asphalt (HMA) have been reported. This may be related to the binder, the mix design, and the aggregate. One solution for limiting these failures is the use of polymers as modifiers for asphalt binder in pavements exposed to severe

climatic conditions and increasingly heavy truck traffic. Although several advantages of polymers have been reported, especially during the last decade, Polymer Modified Binders (PMBs) have not yet been characterized unambiguously, because of the nature of the binder and the complex interaction between binder and polymer (Isacsson *et al.*, 1999). The idea that polymers will result in better long-term performance of the binder is a too simple view of a very complex situation. Unless rheologists can define the suitable type of polymer for each application and the suitable extent of the modification, actual effects of polymer on binder performance would be left to chance.

The use of Polymer Modified Binders is increasing rapidly throughout the world. In France, trial strips were made as early as 1963 (Laboratoire Central, 1963). Their purpose was to determine the behavior of modified asphalt by introducing different natural or synthetic rubbers. The results were not considered promising enough to warrant further development (Brule, 1996). However, polymer capability did prove to enhance binder performance and by 1993, more than 8% of the binders used for road applications in France were PMBs. The use of PMBs reached 6% to 7% in Germany and Poland, and values were slightly lower in other European countries (Bonemazzi *et al.*, 1996).

#### 2.4.1. Polymer Modifiers

Polymers are long-chain molecules of very high molecular weight often measured in hundreds of thousands (Sperling, 1992). Polymers used by the binder industry are classified based on different criteria. One method classifies polymers into two general categories: elastomers and plastomers. The mechanism of resistance to deformation is different between elastomers and plastomers. The load-deformation behavior of elastomers is similar to that of a rubber band, i.e., increasing tensile strength with increased elongation and ability to recover to the initial state after removal of load. Under a given load, elastomers deform faster than plastomers, gain more strength during elongation, and recover elastically after withstanding large strains. Plastomers, on the other hand, exhibit high early strength but are less flexible and more prone to fracture under high strains than elastomers. Examples of polymers widely used in flexible pavements are the thermoplastic rubbers, styrene-butadiene-styrene (SBS), an elastomer, and ethylene vinyl acetate (EVA), a plastomer.

In this study, only elastomeric modifiers were considered due to their widespread use in the asphalt industry and their ease in mixing and processing in the laboratory. An elastomer may be defined as an amorphous cross-linked polymer above its glass transition temperature (McCrum *et al.*, 1997). Under conditions of constant load, the stretched length decreases on heating and increases on cooling. This is the opposite of the behavior observed for most other materials. The elasticity characteristic of elastomers arises through the entropic straightening and recoiling of the polymer chains. This is an isovolume phenomenon, with Poisson's ratio being close to 0.5. Elastomers follow a non-Hookean behavior; the strain is not proportional to the stress. Elastomers may exhibit an elongation of 1300% of their original length.

The basic equation relating the retroactive stress,  $\sigma$ , of an elastomer in simple extension to its extension,  $\alpha$ , when the original length ( $L_0$ ) is increased to  $L$ ,  $\alpha = L/L_0$ , is given as follows:

$$s = nRT \left( a - \frac{1}{a^2} \right) \quad (2.6)$$

where,

R is the gas constant ( $8.31 \times 10^7$  dynes.cm/mol.K);

T is the absolute temperature (Kelvin); and

n is the number of active network chain segments per unit volume.

There are three main groups of elastomer styrenic block copolymers: styrene-butadiene-styrene (SBS), which is the most commonly used modifier for road applications in its linear grade; styrene-isoprene-styrene (SIS), which is mainly used for hot-melt adhesives; and styrene-ethylene/butylene-styrene (SEBS), which is used for road and roofing applications where high resistance to oxidative and thermal attack is required (Bull *et al.*, 1988).

Elastomers are produced by anionic polymerization using lithium alkyl initiators. The main advantage of this initiator is that it is extremely active and efficient, and can be added in a variety of ways to process a wide range of elastomers. These initiators are added to monomers, the basic building blocks, in a carefully purified hydrocarbon solvent. The lithium alkyls ionize, initiate the reaction and then continue a propagation process whereby the monomers are joined together in chains to form polymers (Figure

2.11). These polymers consist of long chains of the monomer building blocks, sometimes a few hundred, but more frequently between 10,000 and 100,000.

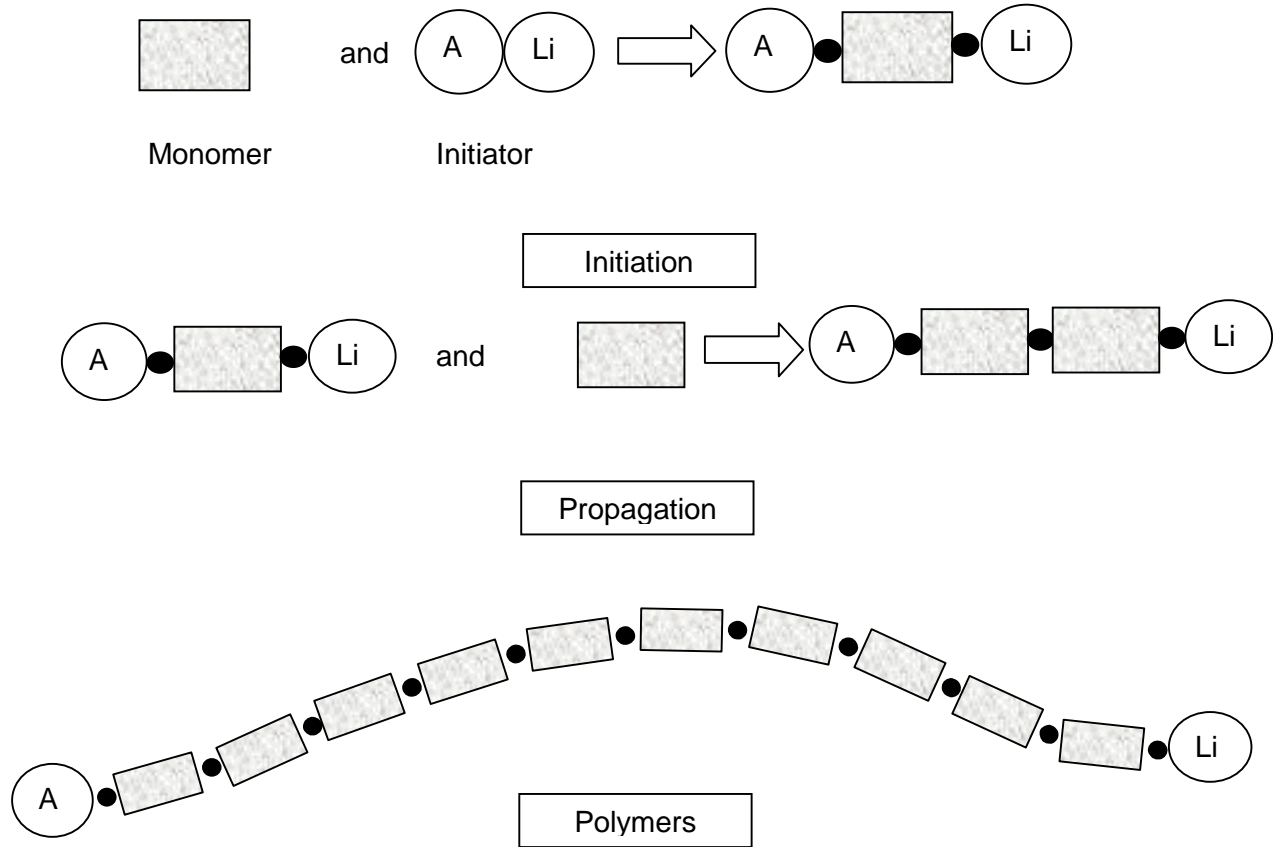


**Figure 2.11.** Lithium Alkyl Polymerization (after Bull *et al.*, 1988)

Polymers produced using one specific monomer are called homopolymers. However, it is possible to produce copolymers or polymers with a chain structure containing more than one monomer by changing the monomer during the polymerization.

By beginning the solution polymerization with styrene monomer, then switching to a butadiene or isoprene feedstock during the course of the polymerization, and finally reverting to styrene, it is possible to make a butadiene rubber (BR) or isoprene rubber (IR) tipped at each end with polystyrene (PS). This elastomer is a copolymer that is characterized by two different glass transition temperatures ( $T_g$ ). This indicates a single copolymer composed of two chemically united, but very different polymers, the rubbery one having a  $T_g$  of  $-90^\circ\text{C}$ , and the hard glassy one having a  $T_g$  of  $+100^\circ\text{C}$ .

#### 2.4.2. Polymer-Binder Mixing Process

When a binder is mixed with a thermoplastic polymer in a hot environment, one of the following three mixes result (Brule, 1996):

- *The mix is heterogeneous:* this is the most frequent scenario where the polymer and the binder prove to be incompatible. In this case, the constituents in the mix separate and the mix has none of the characteristics of a road binder.
- *The mix is totally homogeneous:* this is an unusual case of perfect compatibility. In this case, the oils in the binder solvate the polymer perfectly and destroy any intermolecular interactions. The mix is extremely stable, but the modification to the binder performance is almost negligible; only its viscosity increases. This case should be avoided.
- *The mix is microheterogeneous:* in this case, the blend is made up of two distinct finely interlocked phases. This is the degree of compatibility sought because it significantly enhances the performance of the binder.

When mixed with asphalt binder, elastomers form a two-phase system at service temperature, with one phase containing nearly all the polymer and the other phase containing nearly all the asphaltenes (Shell Chemicals, 1995). Blended with a concentration between 3% to 6% by weight, the swollen polymer becomes the major component in the blend (Bull *et al.*, 1988). The two-phase system is composed of an asphaltene-rich phase (ARP) and a polymer-rich phase (PRP). These two phases differ widely in their rheological and chemical properties (Iscasson *et al.*, 1999). Earlier research has shown that polymers are able to absorb the maltenes from the asphalt binder to form a dominant phase that is soft, flexible, and elastic. This continuous phase largely governs the blend properties. On the other hand, the asphaltene-rich phase is hard, brittle, and non-elastic (Shell Chemicals, 1995).

Since a modified binder consists of two distinct phases, three different cases may occur:

- The polymer content is low (less than 4%): in this case, the bitumen is the continuous phase of the system, and the polymer is dispersed through it. With its

lowered oil content, the binder phase has a correlatively higher asphaltene content; as a result, its cohesion and elasticity are both enhanced.

- The polymer content is sufficiently high (more than 7%): in this case, the properties of the mix are completely different from those of the binder. The blend would behave as a thermoplastic adhesive rather than a polymer-modified binder.
- The polymer content is around 5%: this may form microstructures in which the two phases are continuous and interlocked; such systems are generally difficult to control and present stability problems (Brule, 1996).

## **2.5. LINEAR VISCOELASTIC THEORY**

When a stress or a strain is impressed upon a body, rearrangements take place inside the material by which it responds to the imposed excitation. In any real material these rearrangements necessarily require a finite time. The time required, however, may be very short or very long (Tschoegl, 1989). When the material rearrangements take virtually infinite time, the material is called a purely elastic material. Strain response of a linear elastic material to arbitrary stress input is not time dependent and is in phase with the applied stress. In other words, under a constant suddenly applied load, an elastic material will deform instantaneously, maintain constant deformation, and upon removal of the load return to its initial shape. When the material rearrangements take place so rapidly that the time is negligible compared with the time scale of the experiment, we regard the material as purely viscous. In a linear viscous material, the strain response is time dependent and out of phase with respect to the stress input. If subjected to a constant instantaneous load, the viscous material does not show immediate response, undergoes an increasing deformation with constant rate, and when the load is removed will maintain its deformed shape. Water comes close to being a purely viscous material and steel, if deformed to no more than 1% or 2%, behaves in an almost completely elastic fashion. The classical theories of linear elasticity and Newtonian fluids, though impressively well-structured, do not adequately describe the response behavior and flow of most real materials (Haddad, 1995). Attempts to characterize the behavior of such real materials under the action of external loading led to focus on the material's rheology and thus what is known as 'viscoelasticity'. In a

typically viscoelastic material, the time necessary for the material rearrangements to take place is comparable with the time scale of the experiment.

Asphalt binder is a viscoelastic, thermoplastic, rheodictic material that is characterized by a certain level of rigidity of an elastic solid body, but, at the same time, flows and dissipates energy by frictional losses as a viscous fluid. As any viscoelastic material, asphalt's response to stress is dependent on both temperature and loading time. An overview of the viscoelastic theory is presented in the following subsections.

### 2.5.1. Constitutive Models

In order to predict the engineering performance of any material, it is necessary to understand its stress-strain behavior. The stress-strain behavior of viscoelastic materials in uni-axial stress closely resembles that of models built from discrete elastic and viscous elements. The following models may be used to describe viscoelastic materials and to establish their differential equations.

#### 2.5.1.1. The Basic Elements: Spring and Dashpot

Consider a helical spring (Figure 2.12a). When a force  $P$  is applied, the length of the spring increases by a certain amount  $\Delta l$ , and when the force is removed, the spring returns to its original length. If the material is linear-elastic, the following relation is valid:

$$s = Ee \quad (2.7)$$

where,

$\sigma$  is the applied stress;

$E$  is the elasticity modulus; and

$\epsilon$  is the resulting strain.

Now consider the "dashpot" (Figure 2.12b). A piston is moving in a cylinder with a perforated bottom so that no air is trapped inside. Between the cylinder and the piston wall there is a rather viscous lubricant so that a force  $P$  is needed to displace the piston. The stronger this force, the faster the piston will move. However, in this case, it is not its elongation that is proportional to the force, but its time rate of change. The relation between stress and strain is expressed as follows:

$$\tau = \eta \dot{\gamma} \quad (2.8)$$

where,

$\tau$  is the applied shear stress;

$\eta$  is the viscosity coefficient; and

$\dot{\gamma}$  is the shear strain rate.

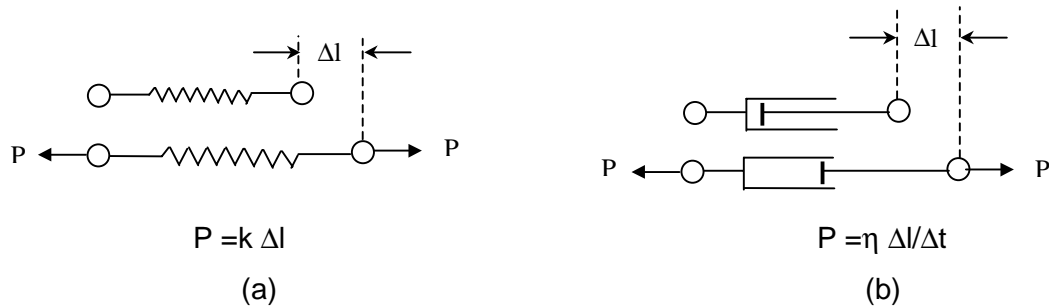


**Figure 2.12.** The Basic Elements Used to Explain Elastic and Viscous Behavior (a) Spring and (b) Dashpot

The behavior of viscoelastic materials is a mixture of the two simple cases described in Figure 2.12. More complicated models can be built by combining springs and dashpots, which can describe possible patterns of the viscoelastic behavior. Whether a given material performs according to one or another of these models is a question to be resolved by testing. If it does, the model is validated.

### 2.5.1.2 The Governing Differential Equation (GDE)

The following linear differential relation is used as a linear viscoelastic constitutive equation relating the stress to strain:

$$P\sigma(t) = Q\varepsilon(t) \quad (2.9)$$

where P and Q are linear differential operators with respect to the time t. In a general form, these operators are expressed as follows:

$$\begin{aligned} \mathbf{P} &= \sum_{i=0}^p a_i \frac{\partial^i}{\partial t^i} \\ \mathbf{Q} &= \sum_{i=0}^q b_i \frac{\partial^i}{\partial t^i} \end{aligned} \quad (2.10)$$

where  $a_i$  and  $b_i$  are material constants. The number of the constants  $a_i, b_i$  depends on the viscoelastic response of the particular material under consideration. By reducing equations 2.9 and 2.10, the following equation results:

$$a_0 \mathbf{S} + a_1 \frac{d\mathbf{S}}{dt} + a_2 \frac{d^2 \mathbf{S}}{dt^2} + \dots = b_0 \mathbf{e} + b_1 \frac{d\mathbf{e}}{dt} + b_2 \frac{d^2 \mathbf{e}}{dt^2} + \dots \quad (2.11)$$

It may be sufficiently accurate for binders to represent the viscoelastic response over a limited time scale by considering only one or two terms on each side of Equation 2.11. This would then be equivalent to describing the linear viscoelastic behavior by mechanical models constructed of linear elastic elements, which obey Hooke's law, and viscous dashpots, which obey Newton's law of viscosity. By considering the reference strain to be at  $t=0$ , the simplicity given by the Laplace Transformation may be utilized. The manipulation of differential, integral, or integro-differential equations is greatly facilitated by the use of Laplace Transformation. Using this technique, a differential equation with constant coefficients in the *time* domain becomes an algebraic equation in the *complex* domain. This equation may be manipulated algebraically and the result can then be retransformed into the real time domain. To achieve this goal, two simple rules need to be followed:

1. The Laplace Transformation for any function ( $\sigma, \epsilon \dots$ ) is noted as  $(\bar{\sigma}, \bar{\epsilon} \dots)$ , which represents its transform  $\bar{f}(s)$ .
2. The  $n^{\text{th}}$  derivative of  $f(t)$  has its Laplace transform  $s^n \bar{f}(s)$  (e.g.  $(\mathcal{L} \dot{\epsilon}) = s\bar{\epsilon}$ ).

Hadad (1995) and Tschoegl (1989) provide a complete treatment of Laplace Transformations. Transformation of the operator equation leads to:

$$\bar{u}(s) \bar{\mathbf{S}}(s) = \bar{q}(s) \bar{\mathbf{e}}(s) \quad (2.12)$$

where  $\bar{\mathbf{s}}(s)$  and  $\bar{\mathbf{e}}(s)$  are the stress and strain transforms and  $\bar{u}(s)$  and  $\bar{q}(s)$  are the linear differential operators in Laplace domain, respectively. From equation 2.12, the following is obtained:

$$\bar{\mathbf{s}}(s) = \bar{Q}(s)\bar{\mathbf{e}}(s) \quad \text{and} \quad \bar{\mathbf{e}}(s) = \bar{U}(s)\bar{\mathbf{s}}(s) \quad (2.13)$$

Equation 2.13 will form the basis of the viscoelastic modeling of asphalt binder in this study.  $\bar{Q}(s)$  and  $\bar{U}(s)$  are the operational (shear) *relaxance* and *retardance*, respectively (Fluge, 1967). They will be referred to as the respondances. The main benefit of the relaxance is that it facilitates more complicated models by the help of its electromagnetic analogy with the impedance. From Equation 2.13,

$$\bar{Q}(s)\bar{U}(s) = 1 \quad (2.14)$$

Therefore, the operational respondances are reciprocal to each other. This, of course, is not true of the corresponding functions in the time domain,  $Q(t)$  and  $U(t)$ .

### 2.5.1.3. The Harmonic Response Functions

The excitation used in Dynamic Mechanical Analysis (DMA) is the harmonic or sinusoidal steady-state excitation, which is often called dynamic excitation. In this case, either an oscillating stress  $\sigma = \sigma_0 \sin \omega t$  is applied to the material and the strain is measured, or a deformation described by an oscillating strain is applied and the stress is measured. Instead of assuming the strain to vary like a sine or cosine of time, it will be advantageous to handle both forms of the excitation simultaneously using its complex form:

$$\varepsilon(t) = \varepsilon_0(\cos \omega t + i \sin \omega t) = \varepsilon_0 e^{i\omega t} \quad (2.15)$$

where,

$\varepsilon_0$  is the strain amplitude; and

$\omega$  is the radian frequency.

In the steady-state case, the variable of interest is no longer the time  $t$  because the response will vary with  $t$  in a periodic manner. The response will, however, vary with the frequency of the periodic excitation that therefore becomes the variable of interest in the steady state. It can then be shown that in the case of the radian frequency as variable of interest, the following equation results:

$$\sigma(\omega) = \bar{Q}(i\omega)\varepsilon(\omega) = G^*(\omega)\varepsilon(\omega) \quad (2.16)$$

The quantity  $\bar{Q}(i\omega)$  has the dimensions of a modulus. In polymer mechanics, it is usually denoted by  $G^*(\omega)$  and is called the complex shear modulus. From the previous equation, the complex shear modulus is defined as the sinusoidal steady-state stress response to a sinusoidal steady-state strain of unit amplitude (Tschoegl, 1989).

#### 2.5.1.4. Relations between Standard Response Functions Associated with Creep and Relaxation

It is seen from Equations 2.11 and 2.12 that description of linear viscoelastic behavior by linear differential equations with constant coefficients leads to operational respondances, which are ratios of polynomials in the transform variable  $s$ . In binder rheology, interest is mainly on the complex shear modulus that can be directly obtained from the respondances (relaxance and retardance) as any other standard response functions. The relations listed in Table 2.4 are used extensively in this study.

**Table 2.4.** Response to the Standard Stimuli (after Tschoegl, 1989)

From $\bar{U}(s)$	From $\bar{Q}(s)$
$J(t) = L^{-1} \bar{U}(s) / s$	$G(t) = L^{-1} \bar{Q}(s) / s$
$J^*(\omega) = [\bar{U}(s)]_{s=j\omega} = \bar{U}(j\omega)$	$G^*(\omega) = [\bar{Q}(s)]_{s=j\omega} = \bar{Q}(j\omega)$
$J'(\omega) = \text{Re } \bar{U}(j\omega)$	$G'(\omega) = \text{Re } \bar{Q}(j\omega)$
$J''(\omega) = -\text{Im } \bar{U}(j\omega)$	$G''(\omega) = -\text{Im } \bar{Q}(j\omega)$
$\tan \delta(\omega) = J''(\omega) / J'(\omega)$	$\tan \delta(\omega) = G''(\omega) / G'(\omega)$

### 2.5.1.5 Electromechanical Analogies

Earlier, analogies were made between electrical networks and mechanical models. Because of the ease with which electrical networks can be built and analyzed, and because of the advanced state of electrical circuit analysis, other physical systems, such as mechanical, acoustic, or hydraulic, are often represented and analyzed in terms of their electrical analogs (Gardner *et al.*, 1953).

This analogy allows the derivation of the GDE governing the behavior of the model in hand by node analysis. This makes use of the *combination rules* that state that relaxances add in parallel, and retardances add in series.

### 2.5.1.5 The Maxwell and Voigt Units

For the basic elements previously presented, it can be shown using Equations 2.7 and 2.8 that for a spring,  $\bar{\mathbf{S}}(s) = G\bar{\mathbf{e}}(s)$  in Laplace domain where  $G$  is the shear modulus, and for a dashpot,  $\bar{\mathbf{S}}(s) = h\dot{\bar{\mathbf{e}}}(s)$ . This simple relation may be used to investigate more complicated combination of springs and dashpots that might describe some of the viscoelastic behavior.

For the Maxwell unit presented in Figure 2.13a, retardance of this model can be easily obtained using the combination rules as

$$\bar{\mathbf{U}}(s) = J + \mathbf{f}/s \quad (2.17)$$

where  $J$  is used for  $1/G$  and  $\phi$  for  $1/\eta$ . Hence,

$$\bar{\mathbf{e}}(s) = (J + \mathbf{f}/s)\bar{\mathbf{S}}(s) \quad (2.18)$$

By inverting the previous equation, the relaxance can be obtained as

$$\bar{\mathbf{Q}}(s) = \frac{1}{\frac{1}{G} + \frac{1}{hs}} \quad (2.19)$$

Introducing the relaxation time as

$$t_M = h / G \quad (2.20)$$

Equation 2.20 can be written as

$$\bar{Q}_M(s) = \frac{G t_M s}{1 + t_M s} \quad (2.21)$$

For the Voigt unit presented in Figure 2.13b, all parallel elements experience the same strain, and the stresses in these elements are additive. Using the combination rules that relaxances add in parallel and retardances add in series, the following results:

$$\bar{Q}(s) = G + h s \quad (2.22)$$

The retardance, which is the inverse of the relaxance, can be written as follows:

$$\bar{U}(s) = \frac{1}{G + h s} \quad (2.23)$$

Neither model by itself represents viscoelastic behavior adequately. These units are, however, important building blocks for other more complex models. A viscoelastic material shows both retardation of strain (i.e. creep) as expressed by the Voigt unit and relaxation of stress as expressed by the Maxwell unit.

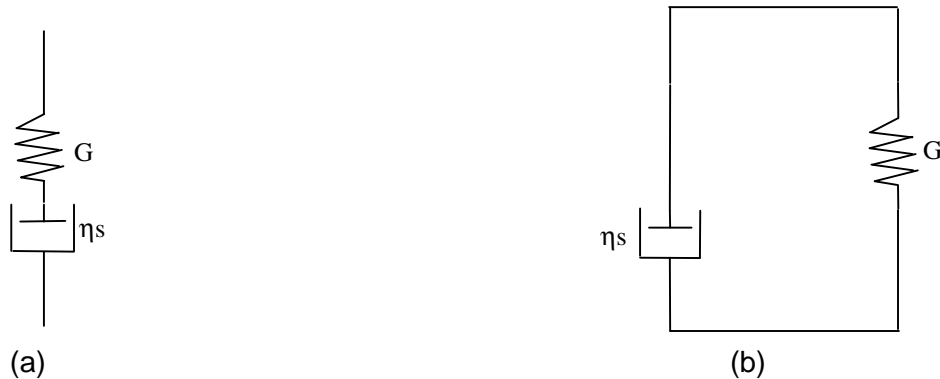


**Figure 2.13.** The Maxwell (a) and Voigt (b) Units

An adequate model for representing a solid-like linear viscoelastic behavior requires a minimum of three elements (two-springs and one dashpot), while liquid-like behavior must be modeled by no less than four elements (two springs and two dashpots). The addition of a spring, a dashpot, or another Voigt unit in parallel to a Voigt unit, or a spring, a dashpot, or another Maxwell unit in series to a Maxwell unit, does not change the nature of the added-to unit because two elements of the same kind in parallel or in series with each other can always be replaced by a single element of the same kind but different numerical value (Tschoegl, 1989). Hence, the add is always to a Voigt unit in series and to a Maxwell unit in parallel.

### 2.5.2 Continuous Time Spectra

The time domain is assumed to be restricted to the interval between zero and infinity. This assumption is valid, as the state in which the material is at  $t=0$  is the reference state, and the material is free of the effects of any stress or strain history it might have experienced prior to  $t=0$ . The preferred configuration is when the reference state is the undeformed state. Such material will be termed *arrheodictic*. By contrast, most common liquids, including viscoelastic ones, are *rheodictics*. Such materials do not have a preferred configuration and it makes no sense to talk about an undeformed state. For a generalized Maxwell model (see Figure 2.14) describing arrheodictic behavior, with the help of Equation 2.21, it can be shown that the relaxance can be written as follows:

$$\bar{Q}(s) = G_e + \sum_n \frac{G_n \tau_n s}{1 + \tau_n s} \quad (2.24)$$

where,

$\tau_n$  is the relaxation time corresponding to the  $n$  Maxwell element (sec);

$G_e$  is called the equilibrium shear modulus corresponding to the first spring (Pa); and

$G_n$  is the shear modulus corresponding to the  $n$  Maxwell element (Pa).

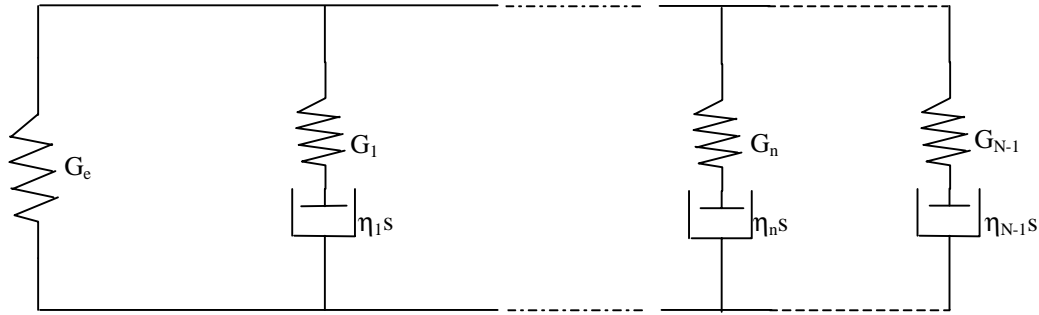


**Figure 2.14.** Generalized Maxwell Model Describing Arrheodictic Behavior

This model represents arrheodictic behavior, as it has an equilibrium modulus ( $G_e$ ), which is the shear modulus of an extra isolated spring added in parallel to the generalized model. The number  $n$  denotes the number of Maxwell elements arranged in parallel. Although experimental data shows that asphalt has no preferred undeformed state ( $G_e=0$ ), the general arrheodictic case is usually presented.

If the finite number of elements  $n$  in the generalized Maxwell model is replaced by an infinite number (spectrum) of elements, using Equation 2.24, the relaxance will be defined as follows:

$$\bar{Q}(s) = G_e + \int_{-\infty}^{\infty} H(\tau) \frac{\tau s}{1 + \tau s} d \ln \tau \quad (2.25)$$

where  $H(\tau)$  is called the relaxation spectrum. The differential,  $d \ln \tau$ , may be considered to be a shorthand symbol for  $d\tau/\tau$ . It is sometimes useful to replace it by  $d\tau/\tau$ , changing the lower limit of integration from  $-\infty$  to zero. Using Table 2.2, the various experimental functions may be obtained from the relaxance  $\bar{Q}(s)$  and the retardance  $\bar{U}(s)$ , which yield to an integral over the continuous spectral distribution functions  $H(\tau)$  multiplied by a certain kernel function characteristic of the time regime of the stimulus which elicited the response. For the case of an harmonic response function, it can be shown that the complex shear modulus ( $G^*$ ) can be written as follows:

$$G^*(\omega) = G_e + \int_{-\infty}^{\infty} H(t) \frac{j\omega t}{1 + j\omega t} d \ln t \quad (2.26)$$

Response functions written in terms of the spectra are said to be expressed in the functional *canonical representation* (Tschoegl, 1989). This means that every given value of a response function depends on all values of the spectral function over its entire domain of definition from  $\tau=0$  to  $\tau=\infty$ .

The relaxation spectrum cannot be obtained directly by any experiment (Ferry, 1980). It must be extracted by mathematical means from the integral part of equation 2.25. Several methods for obtaining approximations to the spectra by solving the integral equations have been suggested but have not been well received (Tschoegl, 1989). Hence, such methods will not be discussed here. Instead, approximations to the spectra by using mathematical models will be examined.

From Table 2.2, the transform of equation 2.25 leads to the relaxation modulus  $G(t)$ :

$$G(t) = G_e + \int_{-\infty}^{\infty} H(t) e^{(-t/\tau)} d \ln \tau \quad (2.27)$$

Another expression for the relaxation modulus that is sometimes useful is

$$G(t) = G_g - \int_{-\infty}^{\infty} H(\tau) [1 - e^{(-t/\tau)}] d \ln \tau \quad (2.28)$$

where,

$G_g$  is the glassy shear modulus (Pa).

Subtracting equation 2.28 from equation 2.27 leads to the following expression:

$$G_g - G_e = \int_{-\infty}^{\infty} H(\tau) d \ln \tau \quad (2.29)$$

## 2.6. COMPLEX SHEAR MODULUS MASTER CURVES

Two issues must be dealt with in describing the rheological behavior of asphalt binders: time dependency and temperature dependency. The common approach is to reduce the three-dimensional problem to a two-dimensional problem by imposing the time-temperature superposition principle that was introduced by Tobolsky (1956) and theoretically validated based on the Williams-Landel-Ferry (WLF) equation (Ferry, 1980). The WLF equation expresses a logarithmic relationship between time and temperature. Building on these ideas, the time-temperature superposition principle states that with viscoelastic materials, time and temperature are equivalent to the extent that data at one temperature can be superimposed on data at another temperature by shifting the curves along the time axis (Tobolsky, 1956). The power of the WLF equation lies in its generality and derivation that is based on the free volume theory.

As first developed by Eyring (1938), molecular motion in the bulk state depends on the presence of holes, or places where there are vacancies or voids. When a molecule moves into a hole, the hole exchanges places with the molecule. When describing polymer motion, more than one hole may be required to be in the same locality. Thus, for a polymeric segment to move from its present position to an adjacent site, a critical void volume must first exist before the segment can jump. These holes are called free volume.

Fox and Flory (1954) defined the specific free volume,  $n_f$  as follows:

$$n_f = K + (a_R - a_G)T \quad (2.30)$$

where,

$n_f$  is the specific free volume;

K is related to the free volume at 0°K;

$a_R$  is the cubic volume expansion coefficient in the rubbery state; and

$a_G$  is the cubic volume expansion coefficient in the glassy state.

Based on this concept and early work by Doolittle (1951), the WLF equation is derived in the following form:

$$\log a_T = \log \left( \frac{h}{h_s} \right) = - \frac{C_1 (T - T_s)}{C_2 + (T - T_s)} \quad (2.31)$$

where,

$a_T$  is the shift factor at temperature  $T$ ;

$h$  and  $h_s$  are the Newtonian viscosity at temperature  $T$  and  $T_s$  respectively;

$T_s$  is the reference temperature; and

$C_1$  and  $C_2$  are empirically determined coefficients.

A complete derivation of this principle may be found in Sperling (1992). This principle, also called method of reduced variables (Ferry, 1980) is applicable to linear amorphous polymer above the glass transition temperature ( $T_g$ ). It can be mathematically expressed as given by Gahvari (1996):

$$F(T_1, \omega) = F(T_2, \omega/a_T) \quad (2.32)$$

where,

$F(T_1, \omega)$  is the value of the viscoelastic function at temperature  $T_1$  and frequency  $\omega$ ; and

$F(T_2, \omega/a_T)$  is the value of the viscoelastic function at temperature  $T_2$  and frequency  $\omega/a_T$ .

To apply the time-temperature superposition principle in order to develop master curves, frequency sweeps are performed using the dynamic shear rheometer over a wide range of temperatures and frequencies. To develop a master curve, strong overlap is needed among the curves developed at the different temperatures (Marasteanu *et al.*, 1996). The curve corresponding to one of the temperatures is selected as reference, to which all other temperatures are shifted to build a continuous and smooth curve. The resulting curve extends over a wide range of frequencies and is called a master curve (Figure 2.15).

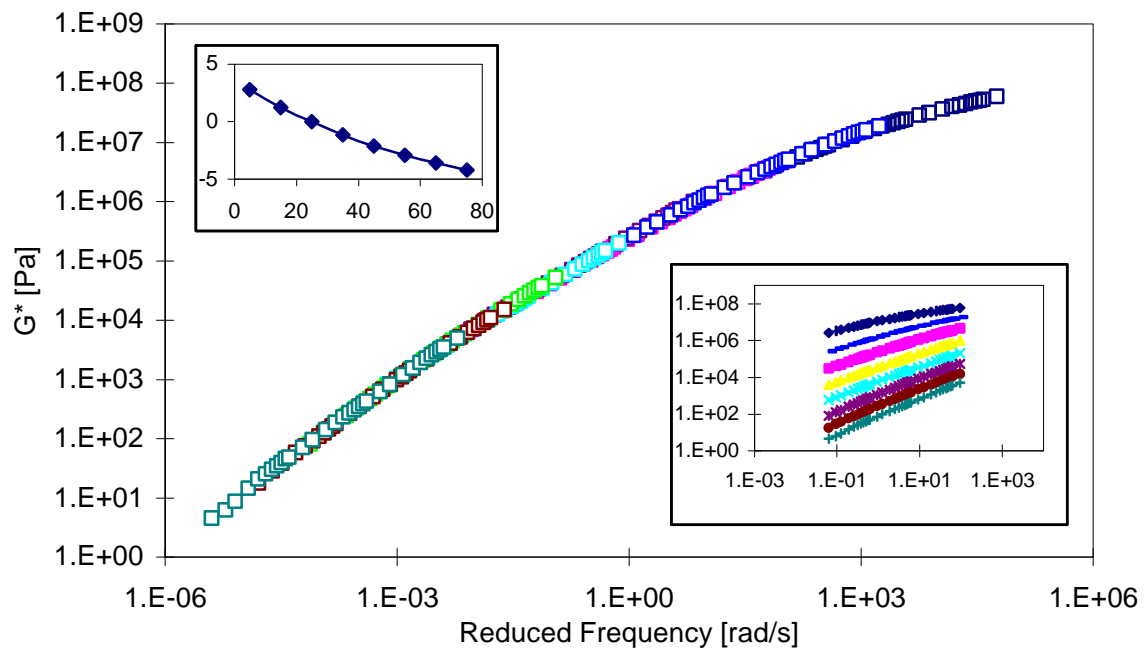


**Figure 2.15.** The Making of a Master Curve

According to Ferry (1980), application of time-temperature superposition principle requires three conditions. First, shapes of adjacent response curves should exactly match. Secondly, the set of shift factors obtained from all viscoelastic functions must be the same. Finally, the variations of shift factors with temperature should follow a rational pattern that is compatible with experience.

Since the introduction of the time-temperature superposition principle to asphalt rheology, many research investigations have been conducted to study the applicability of this principle to asphalt binder (Marasteanu *et al.*, 1996; Lesueur *et al.*, 1997; Attane *et al.*, 1984; Stastna *et al.*, 1997). The feasibility of applying this principle to asphalt binder will be discussed in more detail in Chapter 3.

## 2.7. VISCOELASTIC RESPONSE MODELS OF ASPHALT BINDERS

A quantitative mathematical model that describes the time-temperature dependency of asphalt binders is needed for a number of reasons (see Chapter 1). Since the early fifties, several methods were developed to predict the binder viscoelastic behavior. Most of these models assumed that the time-temperature superposition principle holds for

asphalt binder. The following section provides a quick overview of some of the developed models and their theoretical background.

### 2.7.1. Van der Poel's Nomograph

In 1954, Van der Poel developed a nomograph that could be used to estimate stiffness over a wide range of temperatures and loading times for a variety of binders (then called bitumens). It has been reported that the accuracy of this nomograph to predict the binder behavior is questionable, especially at low temperatures and long loading periods (SHRP, 1994).

### 2.7.2. Jongepier and Kuilman's Model

In 1969, Jongepier and Kuilman derived a mathematical model for frequency dependence of asphalt binders based on the assumption of a log normal distribution for relaxation times. The relaxation spectrum was defined as follows:

$$H(t) = \frac{G_g}{b\sqrt{p}} \exp\left(-\left(\frac{\ln t / t_m}{b}\right)^2\right) \quad (2.33)$$

where,

$b$  is the width of the distribution function;

$t_m$  is the time constant (s); and

$G_g$  is the glassy modulus (Pa).

Based on this distribution function and using Ninomiya and Ferry's approach (Ninomiya *et al.*, 1959), the following equations were derived for the storage and loss moduli, respectively:

$$G'(x) = \frac{G_g}{b\sqrt{p}} \exp\left[-\left(\frac{b(x-1/2)}{2}\right)^2\right] \int_0^{\infty} \exp\left(-\left(\frac{u}{b}\right)^2\right) \frac{\cosh(x+1/2)u}{\cosh u} du \quad (2.34)$$

$$G''(x) = \frac{G_g}{b\sqrt{p}} \exp\left[-\frac{b(x-1/2)}{2}\right]^2 \int_0^\infty \exp\left(-\frac{u}{b}\right)^2 \frac{\cosh(x-1/2)u}{\cosh u} du \quad (2.35)$$

where the transformation  $u$  and  $x$  are defined as follows:

$$u = \ln w_r t, \quad (2.36)$$

$$x = \frac{2}{b^2} \ln w_r$$

where  $w_r = \frac{wh_0}{G_g}$  with  $h_0$  representing the Newtonian viscosity (Pa.s).

This approach has the unique advantage of being able to predict the storage and loss components of the shear modulus by two related equations that are in agreement with the theory of linear response. However, mathematical complexity of the equations developed for frequency dependence of response makes their practical application quite difficult. In addition, as stated by the authors, the width parameter,  $b$ , although strongly related to the viscoelastic behavior, is not suitable for rapid characterization of binder.

### 2.7.3. Dobson's Model

In 1969, Dobson made use of shift factors  $a_T$  to plot rheological master curves of asphalts. Based on experimental data performed at temperatures ranging from -10°C to 70°C, he proposed the following equation to fit every master curve versus reduced frequency (Dobson, 1969):

$$\log(G_r^{-b} - 1) = -b \log(w_r) - \frac{20.5 - w_r^{-b}}{230.3} \quad \text{when } w_r > 10^{-1/b} \quad (2.37)$$

$$\log G_r = \log \omega_r \quad \text{when } \omega_r < 10^{-1/b} \quad (2.38)$$

where,

$G_r$  is the relative complex shear modulus defined as  $G_r = G^*(\omega)/G_g$  with  $G_g$  being the glassy modulus;

$\omega_r$  is defined as  $\omega_r = a_T \eta_0 \omega / G_g$  with  $\eta_0$  being the zero-shear viscosity; and

$b$  is a parameter that measures the width of the relaxation spectrum.

Based on experimental observations, the following relationship between complex modulus and loss tangent for values of  $\tan \delta < 9.5^\circ$  was proposed:

$$\frac{d \log |G^*|}{d \log \omega} = \frac{\tan \mathbf{d}}{(1 + \tan \mathbf{d})(1 - 0.01 \tan \mathbf{d})} \quad (2.39)$$

#### 2.7.4. Dickinson and Witt's Model

In 1974, Dickinson and Witt, based on dynamic mechanical data on 14 different binders, developed two analytical expressions for complex shear modulus and phase angle in terms of frequency. The resulting equation defines the relative shear modulus in terms of relative frequency:

$$\log G_r = \frac{1}{2} \left[ \log \mathbf{w}_r - \sqrt{(\log \mathbf{w}_r)^2 + (2\mathbf{b})^2} \right] \quad (2.40)$$

where,

$$\mathbf{w}_r = \frac{h_0 \omega a_T}{G_g} \quad (2.41)$$

$$G_r = \frac{|G^*|}{G_g} \quad (2.42)$$

where,

$a_T$  is the shift factor;

$G_g$  is the glassy shear modulus (Pa);

$\omega_r$  is the relative frequency;

$\eta_0$  is the Newtonian viscosity (Pa.s);

$G_r$  is the relative shear modulus;  
 $\omega$  is the reduced frequency in (rad/s); and  
 $\beta$  is the shear susceptibility parameter.

The shear susceptibility parameter,  $\mathbf{b}$ , varies based on composition and aging condition of binder.

The mathematical expression for the phase angle  $\mathbf{d}$  is as follows:

$$\mathbf{d} = \mathbf{d}' + \frac{\mathbf{p} - 2\mathbf{d}'}{4} \left[ 1 - \frac{\log \mathbf{w}_r}{\sqrt{(\log \mathbf{w}_r)^2 + (2\mathbf{b})^2}} \right] \quad (2.43)$$

where,

$\delta$  is the phase angle; and

$\mathbf{d}'$  is a small angle (less than 3°) that is assigned to the glassy modulus.

In general, the above model appears to be somewhat simpler, and of similar or better accuracy, than Jongepier and Kuilman's (SHRP, 1994). Dickinson and Witt reported a strong relationship between  $G_g$  and  $\mathbf{b}$  when using their model. However, the reported values of  $\log G_g^*$  ranged from 8 to 9.6 Pa, which is considerably different from the more or less constant value of 9 Pa reported by other researchers (Van der Poel, 1954; Pink *et al.*, 1980). This may suggest inaccuracy in both the glassy modulus and  $\mathbf{b}$  parameters determined by their model (SHRP, 1994).

#### 2.7.5. Christensen and Anderson's Model

In 1992, Christensen and Anderson presented a mathematical model after performing dynamical mechanical analysis on the eight SHRP core binders. The mathematical model was derived based on a logistic distribution function for the resulting relaxation spectra. The following equations were proposed to define the complex moduli and phase angle in terms of frequency:

$$|G^*(\omega)| = G_g \left[ 1 + \left( \frac{\omega_c}{\omega} \right)^{\frac{\log 2}{R}} \right]^{-\frac{R}{\log 2}} \quad (2.44)$$

$$d(\omega) = \frac{90}{1 + \left( \frac{\omega}{\omega_c} \right)^{\frac{\log 2}{R}}} \quad (2.45)$$

where,

$\omega_c$  is the crossover frequency (rad/sec); and

R is the rheological index defined by  $\log \left( \frac{G_g}{|G^*(\omega)|} \right)_{\omega=\omega_c}$ .

This mathematical model turned out to be a simplified Dobson model, with  $R=(\log 2)/b$  (Lesueur *et al.*, 1997). The parameters  $\omega_c$  and R in this model have physical significance. The crossover frequency,  $\omega_c$ , represents the frequency at which  $d = 45^\circ$ . Several observations have confirmed that this frequency usually coincides with the intersection of glassy and viscous asymptotes of the modulus master curve. The rheological index, R, on the other hand, is a shape parameter for the master curve and represents the width of the relaxation spectrum. The phase angle formulation is simply a Cole-Cole function, except that the numerator is 90 instead of unity (Marasteanu *et al.*, 1999). This model has a simpler shape than the previous models. However, through comparison of the experimental data on those generated by the model, the authors observed some discrepancy for moduli below about  $10^5$  Pa. Thus, the use of this model may be strictly suitable for characterizing the response at intermediate and high ranges of modulus.

#### 2.7.6. Gahvari's Model

In 1995, Gahvari conducted an experimental program to characterize the dynamic mechanical properties of polymer modified asphalt binders at intermediate and high temperatures. He presented two models for the storage and loss moduli:

$$\log G'(\omega) = \log G_g \left[ 1 - \left( \frac{e^{-1}}{\omega^{\log_e}} \right)^p \right] \quad (2.46)$$

where,

$l$  is the location parameter for the master curve =  $\log \frac{1}{\omega} \Big|_{G'=1}$  ; and

$p$  is the proportionality factor.

$$\log G''(\omega) = (\log \omega + d) - \sqrt{(\log \omega - \log \omega_d)^2 + d^2} \quad (2.47)$$

where,

$d$  is half the length of the transverse axis (Pa); and

$\omega_d$  is the location parameter for the master curve (rad/sec) =  $\omega \Big|_{G''=G''_{\max}}$  .

$G''_{\max}$  is the peak value of loss modulus (Pa);

Gahvari reported that the model accuracy was statistically acceptable (Gahvari, 1996). However, deriving two different models that are not related to each other contradicts the theory of linear response that treats the complex shear modulus as a physical function.

#### 2.7.7. Stastna and Zanzotto's Model

In 1996, Stastna and Zanzotto developed a fractional model for the complex modulus based on the assumption that the complex shear modulus for binders can be described by a general power of a rational function (Stastna and Zanzotto, 1996). The model proposed by Stastna and Zanzotto contains an expression describing both the complex shear modulus and the phase angle. The proposed equations for complex shear modulus and phase angle are given by the following:

$$|G^*(\omega)| = h_0 \omega \left\{ \frac{\prod_1^m [1 + (\omega m_k)^2]}{\prod_1^n [1 + (\omega l_k)^2]} \right\}^{1/(n-m)} \quad (2.48)$$

$$d(\omega) = \frac{p}{2} + b \left[ \sum_1^m \arctan(m_k \omega) - \sum_1^n \arctan(l_k \omega) \right] \quad (2.49)$$

where,

$m < n$ ,  $\mu_k > 0$ ,  $\lambda_k > 0$ ,  $\eta_0 > 0$ ;

$\mu_k$  and  $\lambda_k$  represent relaxation times; and

$\eta_0$  is the Newtonian shear viscosity (Pa.s).

This model uses a reduced number of parameters, 10 to 15, compared to some of the more complicated mechanical analog models. However, each of the 10 to 15 parameters in this model is binder specific and must be determined by a statistical regression of the experimental data. When applied to typical data sets, the model was reported to lack statistical robustness because the number of unknown parameters approaches the degree of freedom in the data (Marasteanu *et al.*, 1999).

#### 2.7.8. Marasteanu and Anderson's Model

In 1998, Marasteanu and Anderson modified their 1992 model. They applied the Havriliak and Negami model to the complex shear modulus, resulting in the following expression (Marasteanu *et al.*, 1999):

$$|G^*(\omega)| = G_g [1 + (\omega_c / \omega)^v]^{-\frac{w}{v}} \quad (2.50)$$

where,

$\omega_c$  is the crossover frequency (rad/sec);

R is the rheological index defined by  $\log \left( \frac{G_g}{|G^*(\omega)|} \right)_{\omega=\omega_c}$ ; and

$w$  is a new parameter introduced to this model which was interpreted from the phase angle expression. The phase angle is given by:

$$d(\omega) = 90w / [1 + (\omega_c / \omega)^v] \quad (2.51)$$

where,

$\delta$  is the phase angle; and  $w$  is a new parameter that addresses the issue of how fast or how slow the phase angle converge to the two asymptotes (90 or zero degrees, respectively) as the frequency goes to zero or to infinity. For example, as the frequency approaches zero, a  $w$  larger than one characterizes a binder that reaches the 90 degrees asymptote faster than a binder with a  $w$  value less than one (Marasteanu *et al.*, 1999).

Each of the models described in this section has advantages and disadvantages that are closely related to the means offered at the time of the development. Table 2.3 presents a brief comparison between the models discussed above (after Marasteanu *et al.*, 1996).

## **2.8. MODEL APPLICABILITY TO POLYMER MODIFIED BINDERS**

As presented in the previous section, a variety of one-dimensional competitive models have been used to describe the time and temperature dependency of the moduli of asphalt binders within the region of linear response. Most of the models described in the previous section were developed based on dynamic mechanical data on straight asphalts. Assuming that a model based on straight asphalt binder can adequately describe polymer modified binder simply implies that the introduction of the polymer has no significant effect on the binder performance. Indeed, polymers have a significant effect on binder performance (Gahvari *et al.*, 1996; Airey *et al.*, 1998; Brule, 1996).

The thermorheological simplicity of straight asphalts between the glass transition temperature and the Newtonian region has been recognized by different researchers (Brodnyan *et al.*, 1960; Dickinson & Witt, 1974). Most of the research conducted to evaluate the effect of polymers on binder performance indicated that simple blends of binders and polymers generally consist of two-phase mixtures at service temperatures (Vonk *et al.*, 1989). The applicability of the Time-Temperature superposition to such heterophase systems is not certain at this point. In 1996, Gahvari reported that this principle resulted in excellent fit of the experimental data for the construction of master curve (Gahvari, 1996).

**Table 2.5.** Models for Describing Time Dependency of Asphalt Binder (after Marasteanu, 1996)

Model	Year Developed	Asphalt Type	Basic Assumption	Ease of Use	Goodness of Fit
Jongepier Kuilman	1969	Straight	Relaxation spectra follows a log normal distribution.	Poor	Good-limited range
Dobson	1969	Straight	Slope of log complex modulus versus log frequency unique.	Fair	Good-limited range
Dickinson Witt	1974	Straight	A hyperbola describes the complex modulus as a function of temperature.	Fair	Good-limited range
Christensen Anderson	1992	Straight	Logistic distribution function for the resulting relaxation spectra.	Good	Good-wide range- not recommended for phase angle close to 90 degrees
Stastna Zanzotto	1996	Straight and modified	Fractional model assuming that $G^*$ can be described by a general power of a rational function.	Poor*	Good-wide range
Marasteanu and Anderson	1998	Straight and modified	Improvement to the Christensen-Anderson model.	Good	Good-wide range. Some problems at the extremities of response.

\* Author opinion (up to 15 parameters to describe asphalt time dependency).